Tumor cytotoxicity and endothelial Rac inhibition induced by TNP-470 in anaplastic thyroid cancer

Dorit Nahari,[1] Ronit Satchi-Fainaro,[3,4] Ming Chen,[1] Ian Mitchell,[1] Laurie B. Task,[1] Zijuan Liu,[1] Jason Kihneman,[1] Allison B. Carroll,[1] Lance S. Terada,[1,2] and Fiemu E. Nwariaku[1]

Departments of [1]Surgery and [2]Pulmonary Medicine, University of Texas Southwestern Medical Center, Dallas, Texas; [3]Department of Physiology and Pharmacology, Sackler School of Medicine, Tel Aviv University, Tel Aviv, Israel; and [4]Vascular Biology Program, Department of Surgery, Children's Hospital Boston and Harvard Medical School, Boston, Massachusetts

Abstract

Anaplastic thyroid carcinoma is an aggressive form of cancer with no treatment. Angiogenesis inhibitors, such as TNP-470, a synthetic derivative of fumagillin, have been shown to reduce tumor size and increase survival in heterotopic animal models of thyroid cancer. Our goals were to determine the effect of TNP-470 on anaplastic thyroid cancer using an orthotopic murine model, to identify the molecular pathways of TNP-470 actions on endothelial cells, and to determine the non-endothelial tumor effects of TNP-470. We injected human anaplastic thyroid carcinoma cells (DRO′90) into the thyroid glands of nude mice. Mice received TNP-470 (30 mg/kg) s.c. for 6 weeks. TNP-470 prolonged survival and reduced liver metastases. TNP-470 had direct cytotoxic effects on anaplastic thyroid carcinoma cells *in vitro* and *in vivo*. Paradoxically, TNP-470 increased vascular endothelial growth factor secretion from tumor cells *in vitro* and *in vivo.* However, there was no associated increase in tumor microvessel density. In endothelial cells, TNP-470 prevented vascular endothelial growth factor–induced endothelial permeability, intercellular gap formation, and ruffle formation by preventing Rac1 activation. [Mol Cancer Ther 2007;6(4):1329–37]

Received 9/8/06; revised 11/16/06; accepted 2/8/07.

Grant support: American Heart Association grant 0535019N (D. Nahari), Robert Wood Johnson Foundation/Harold Amos Medical Faculty Development Program (F.E. Nwariaku), and NIH grants RO1 GM067674-01A1 (F.E. Nwariaku), R01-HL61897 (L. Terada), and R01-HL67256 (L. Terada).

The costs of publication of this article were defrayed in part by the payment of page charges. This article must therefore be hereby marked *advertisement* in accordance with 18 U.S.C. Section 1734 solely to indicate this fact.

Requests for reprints: Fiemu E. Nwariaku, Department of Surgery, University of Texas Southwestern Medical Center, 5323 Harry Hines Boulevard, Dallas, TX 75390-9156. Phone: 214-648-9968; Fax: 214-648-4784. E-mail: Fiemu.nwariaku@utsouthwestern.edu

doi:10.1158/1535-7163.MCT-06-0554

Introduction

Anaplastic thyroid carcinoma is a locally aggressive and highly metastatic tumor with a median survival of 3 to 4 months. Cure rates of anaplastic thyroid carcinoma are low due to the absence of clinically effective systemic agents for a tumor that is already systemic at the time of presentation (1). Vascular endothelial growth factor (VEGF) is the major proangiogenic factor secreted by tumor cells. VEGF induces proliferation, migration, and survival of endothelial cells, leading to formation of new blood vessels that are essential for tumor growth and metastases. Previous studies show that elevated VEGF levels persist in patients with incomplete resection of thyroid cancer and return to control levels after clinical cure (2, 3). Neoplastic thyroid cells express increased levels of VEGF *in vitro* (2, 4), and patients with thyroid cancer have elevated VEGF levels in both tumors and serum (5, 6). Preclinical studies also show the effectiveness of antiangiogenic agents in thyroid cancer (3, 7). However, the clinical trials will require further examination using clinically relevant animal models. Given the effect of the host microenvironment on tumor response to antiangiogenic therapy, an orthotopic model of thyroid cancer is necessary to study the effectiveness of current antiangiogenic agents (2, 3). Orthotopic animal models of human cancers have the advantage of a relevant tissue microenvironment, which most closely models the human disease (8, 9). This study reports our observations with antiangiogenic therapy in a newly developed orthotopic model of human thyroid cancer. TNP-470 is a synthetic derivative of fumagillin with potent selective effects on endothelial cells *in vitro* (10) and inhibition of tumor growth *in vivo* (11). In clinical trials, TNP-470 slows tumor growth and is associated with complete tumor responses (12). TNP-470 and its polymer conjugate caplostatin each inhibits VEGF-induced endothelial hyperpermeability, causing a decrease in calcium influx and vesiculovacuolar organelle trancytosis (13, 14). However, the mechanisms for the inhibitory effect of TNP-470 on endothelial proliferation and migration are not fully elucidated. Furthermore, the molecular targets for TNP-470 in endothelial and tumor cells are unknown. This information is necessary to better identify which tumors are likely to respond to TNP-470 and to design similar agents in the future. In this study, we show that TNP-470 prolongs survival in an orthotopic model of anaplastic thyroid cancer. We also show that TNP-470 causes tumor cell apoptosis and reduces proliferation. Finally, we report the novel finding that TNP-470 prevents VEGF-induced endothelial cell-cell adhesion, ruffle formation, and cytoskeletal changes, by preventing activation of Rac1, a member of the Rho family of GTPases. We have previously shown that TNP-470 inhibits VEGF-induced endothelial cell migration and RhoA activation (14). Rac

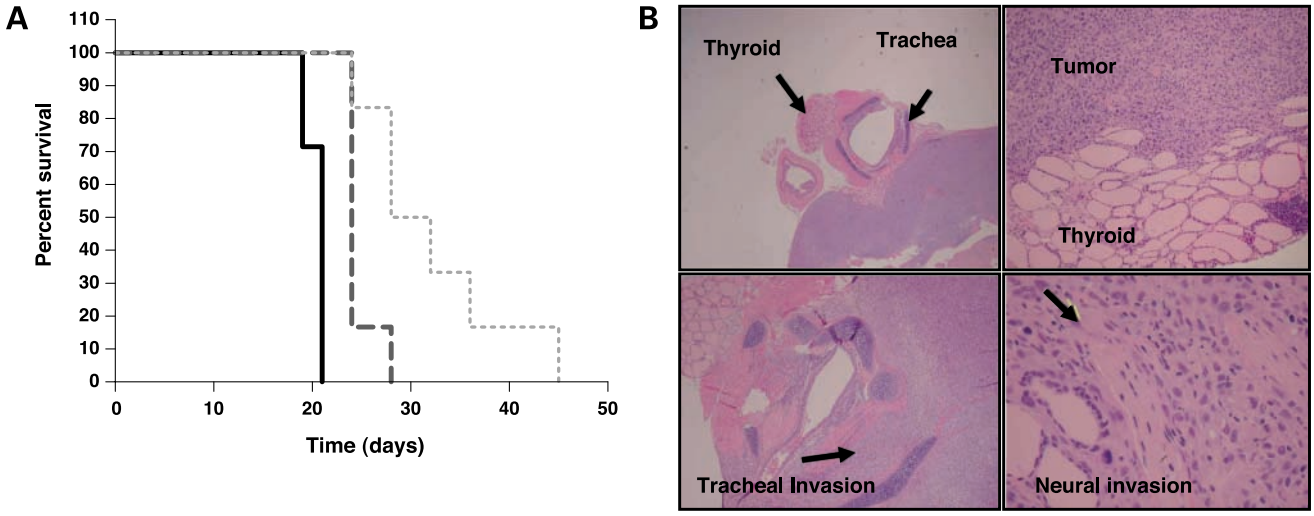

Figure 1. Characterization of orthotopic mouse model for anaplastic thyroid carcinoma. **A,** survival curve for mice injected with DRO'90 cells at the following concentrations: 5×10^4 (*light gray dotted line*), 1×10^5 (*dark gray line*), or 2.5×10^5 (*black line*). End point for curves do not represent death from tumors, but time of euthanasia based on guidelines of the Institutional Animal Care and Use Committee. **B,** H&E staining of anaplastic thyroid tumors showing both neural and tracheal invasion.

has been shown to regulate cytoskeletal reorganization, cell morphology, adhesion, motility, and mitogen-activated protein kinase activation (15) and the integrity of intercellular junctions (16). Here, we extend our findings to implicate the Rac pathway as a mechanism for effects of TNP-470 on endothelial migration and angiogenesis.

Materials and Methods

Cell Lines

Human umbilical vein endothelial cells (HUVEC) were purchased from Cambrex (Walkersville, MD) and cultured in EGM-2 medium (Cambrex). Anaplastic thyroid carcinoma cells were kind gifts from Dr. Guy Juillard (University of California, Los Angeles, CA; DRO'90) and Dr. Kenneth B Ain (University of Kentucky, Lexington, KY; KAT4B). Both cell lines were derived from patients with anaplastic thyroid cancer and have been shown to have several chromosomal abnormalities (17). DRO'90 and KAT4B cells were cultured in RPMI 1640 supplemented with 10% FCS, sodium pyruvate, MEM nonessential amino acid, gentamicin, and 25 mmol/L HEPES (Invitrogen, Carlsbad, CA). Both cell lines were used for *in vitro* experiments (proliferation, caspase assay, and VEGF secretion), whereas only the DRO'90 line was used for tumor injections.

Animal Experiments

Male athymic NCr-*nu/nu* (nude) mice were obtained at 4 to 8 weeks of age (Charles River Laboratories, Wilmington, MA; National Cancer Institute, Bethesda, MD). Mice were fed irradiated 6% mouse chow and water *ad libitum* and handled at all times in a specific pathogen-free environment. Surgical procedures were done under aseptic conditions. All procedures and interventions were approved by the Institutional Animal Care and Use Committee of University of Texas Southwestern Medical Center at Dallas.

Cell Injections

DRO'90 cells were injected as previously described (18). Injection of the thyroid was done in 8- to 12-week-old mice. Mice were anesthetized with i.p. injections of Avertin (tribromoethanol, 1.25 mg/mL). Animals were stabilized in the supine position on a surgical stage with sterile pins. A sterile field was developed by cleaning the surgical site with a Povidone-Iodine Swabstick and 70% alcohol pads. A 1-cm midline cervical incision was made in the neck with the aid of an operating microscope. Submandibular glands and midline strap muscles overlying the trachea were reflected to expose the thyroid lobe. Each mouse was injected with 2.5×10^5 DRO cells in 5 μL of RPMI 1640 in one thyroid lobe, and the skin was closed with stainless steel wound clips. This concentration of cells was based on experiments showing that 2.5×10^5 DRO cells reliably resulted in tumors that were large enough to be visualized and treated within 1 week (Fig. 1A). The animals were allowed to recover from anesthesia while maintained at a constant body temperature with the use of a heating pad. In accordance with Institutional Animal Care and Use Committee policies, buprenorphine hydrochloride was administered as analgesia at a dose of 0.05 to 0.1 mg/kg before complete recovery and repeated after 12 h. Animals were monitored, and surgical staples were removed after 7 to 14 days. All animals were euthanized 6 weeks after injection or after >20% weight loss. In addition, animals that seemed uncomfortable, ill-looking, or in pain before 6 weeks were euthanized immediately. No animals were followed until death. All procedures and protocols were approved by the Institutional Animal Care and Use Committee (APN # 0871-06-03-1). Euthanasia was accomplished using CO_2, after which the entire trachea and tumor were resected *en bloc*. Tumors were divided into

paraffin-embedded blocks or frozen for immunohistochemistry and ELISA. A section of tumor and attached trachea from each animal was stained by H&E to confirm that the tumors were within the thyroid gland. In addition, lungs and liver were harvested. Blood for serum VEGF levels was obtained by cardiac puncture immediately after death.

Interventions

Six days after tumor cell injection, mice were divided into two groups, each of which was treated for 6 weeks as follows: TNP-470 (30 mg/kg) s.c. thrice a week and 200 μL Ringer's Lactate solution (B. Braun Medical, Inc., Irvine, CA) i.p. thrice a week as control group. Body weight and general clinical status of the animals were assessed twice a week.

Immunohistochemistry

Immunohistochemistry was done for cleaved caspase-3 (apoptosis), Ki-67 (proliferation), thyroglobulin (thyroid cell marker), and CD31 (vascular marker). The protocol for immunohistochemistry is as follows: 5-μm-thick paraffin-sectioned slides (Histobond; Statlab, Lewisville, TX) were first heated for 10 min at 55°C. Slides were then deparaffinized with xylene, rehydrated with graded ethanol, and blocked with 3% hydrogen peroxide (Fisher, Houston, TX). For proliferation and apoptosis, tumor sections were stained with mouse antihuman Ki-67 (clone MIB-1; DakoCytomation, Carpinteria, CA) and rabbit anti-human cleaved caspase-3 (Asp^{175}; Cell Signaling Technology, Danvers, MA), respectively. MIB-1 slides underwent heat-induced epitope retrieval with Biocare Medical Reveal in DAKO Pascal pressure cooker. Slides were incubated with 10% goat serum followed by incubation with MIB-1 primary antibody, goat anti-mouse secondary antibody, and streptavidin horseradish peroxidase label were then added. Cleaved caspase-3 was incubated for 60 min at room temperature on a DAKO automated stainer. DAKO Envision dual-link polymer was then applied for 30 min. Finally, DAKO DAB^+ chromogen was applied for 10 min. For thyroid cell staining, tumor sections were stained with mouse anti-human thyroglobulin (DakoCytomation). Immunohistochemistry slides were counterstained with light hematoxylin (Richard Allen, Mayer's hematoxylin) for 3 min and blued in DAKO PBS without Tween. Cryostat sections of the tissues were cut and stained with anti-CD31 for the vasculature. Anti-mouse CD31 (dilution, 1:200; BD PharMingen, San Diego, CA) and peroxidase-conjugated donkey anti-rat IgG (dilution, 1:200; Jackson ImmunoResearch, West Grove, PA) antibodies were used to identify the neovasculature.

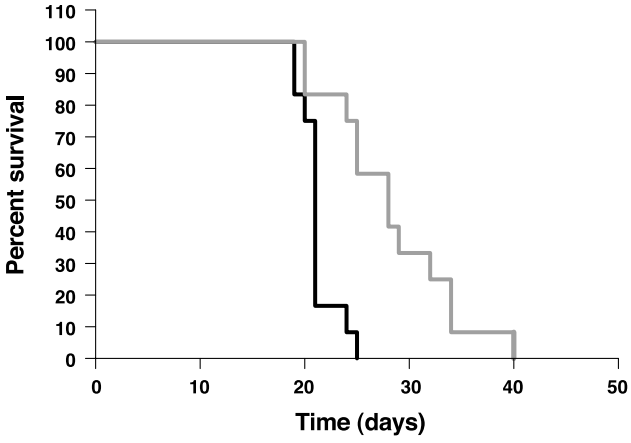

Figure 2. TNP-470 prolongs survival in anaplastic thyroid cancer. Six days after injection of 2.5×10^5 DRO'90 cells, mice were divided into two groups and treated for 6 wks as follows: s.c. TNP-470 (30 mg/kg), 3× a week (*gray line*) and equal volumes of Ringer's Lactate solution, 3× a week as control group (*black line*). TNP-470 significantly prolonged survival ($P < 0.05$).

Serum VEGF Levels

Serum was separated by centrifugation (13,000 rpm, 10 min, 4°C) and stored at −80°C for analysis. Mouse serum VEGF levels were determined using an ELISA kit according to the manufacturer's instructions. (R&D Systems, Minneapolis, MN). Measurement of mouse VEGF levels was done to determine the relative contribution of host (mouse) VEGF secretion from mouse fibroblasts, macrophages, and endothelial cells to tumor growth.

Tumor VEGF Levels

Tumor tissues were homogenized in cell lysis buffer (R&D Systems) at 0°C. Homogenates were frozen and thawed thrice. Soluble protein fraction was separated by centrifugation at 16,000 × *g* for 20 min at 4°C. Protein concentration of the supernatants was measured by Bradford. Lysates were stored at −80°C until used; 200 μg of total lysate was added to each well of a 96-well plate, and human VEGF levels were determined using an ELISA kit according to the manufacturer's instructions. (R&D Systems).

In vitro Tumor Cell VEGF Levels

DRO'90 or KAT4B cells were cultured and then treated with TNP-470 (10 or 20 μg/mL) for 24 h. Human VEGF levels in supernatants were determined using an ELISA kit according to the manufacturer's instructions (R&D Systems).

Caspase-3 Assay

DRO'90 or KAT4B cells were seeded (5×10^6) and then exposed to TNP-470 (10 or 20 μg/mL) for 24 h. Apoptosis was measured using caspase-3/CPP32 colorimetric assay kit (BioVision, Mountain View, CA) according to manufacturer's instructions.

Cell Proliferation

Cell proliferation was assessed using a colorimetric immunoassay kit to quantify incorporation of bromodeoxyuridine during DNA synthesis (Roche Diagnostics, Mannheim, Germany). Briefly, the cells were treated with TNP-470 (20 or 40 μg/mL) for 24 h before assessment of proliferation, and bromodeoxyuridine was added to the cells for 24 h. Fixation and partial DNA denaturation were done before staining with anti-bromodeoxyuridine antibody. Immune complexes were detected by subsequent substrate reaction, and the absorbance at 450 nm was measured using Beckman Coulter AD340 plate reader (Beckman Coulter, Fullerton, CA).

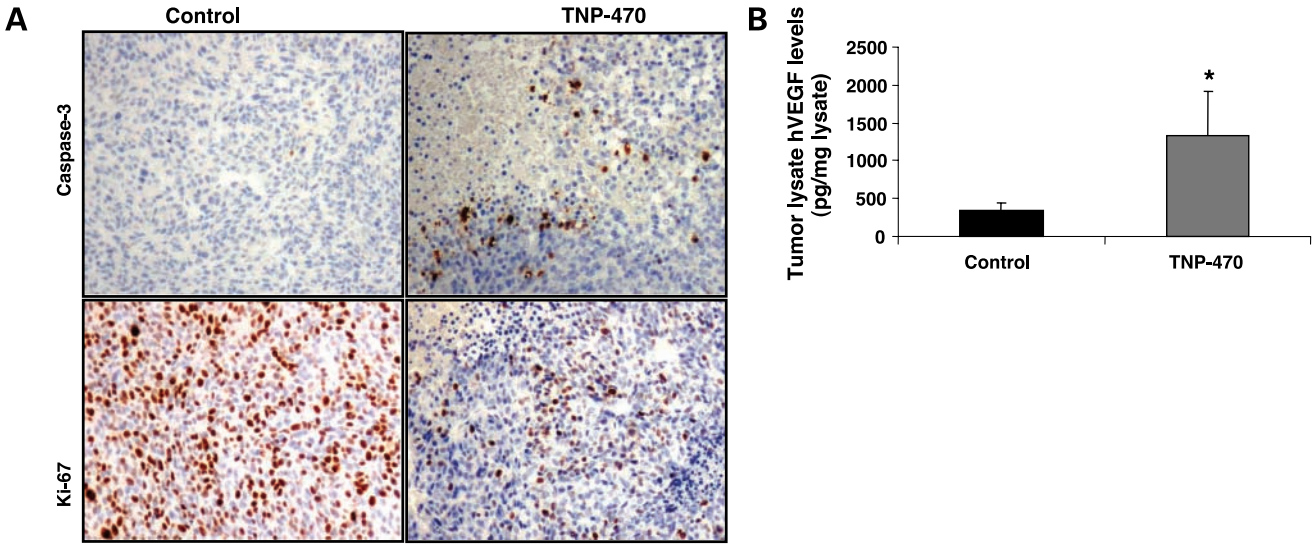

Figure 3. TNP-470 inhibits proliferation, increases apoptosis, and increases VEGF secretion in thyroid tumors *in vivo*. **A,** paraffin-embedded tissues were sectioned, and slides were stained with cleaved caspase-3 antibody to measure apoptosis (*top*) or cell proliferation using Ki-67 antibody (*bottom*). Both sections reveal increased apoptosis and decreased proliferation induced by TNP. **B,** human VEGF levels in DRO tumor lysates were measured by ELISA. TNP increased tumor (human) VEGF secretion. *, $P < 0.05$.

In vitro Endothelial Experiments

Adenoviral Green Fluorescent Protein Constructs and Confocal Microscopy. HUVEC were infected with adenovirus construct coding for the full-length vascular endothelial cadherin-green fluorescent protein (GFP) as previously described (19), or actin-GFP fusion protein (Clontech, Palo Alto, CA) in combination with adenoviral constructs coding for the dominant-negative Rac plasmid, RacN17, or constitutively active RacV12 (a gift from Dr. Kaikobad Irani, Johns Hopkins Medical Center, Baltimore, MD). The following day, cells were starved using EBM medium supplemented by 1% FCS. Twenty-four hours after starvation, the cells were treated with TNP-470 (20 ng/mL) for 2 h followed by VEGF treatment (50 ng/mL). Monolayers were then examined after 30 and 60 min using a Zeiss 410 Axiovert LSM laser scanning confocal microscope (Carl Zeiss, Oberkochen, Germany).

Permeability Assay. VEGF-induced endothelial cell permeability was examined by measuring trans-endothelial monolayer electrical resistance, using an Electric Cell-substrate Impedance Sensing, ECIS system (Applied BioPhysics, New York, NY). Confluent HUVEC were cultured using EGM-2 medium supplemented with 2.5 mg/mL HBOC-201 (Biopure Corp., Cambridge, MA) in specialized wells (Applied BioPhysics) and exposed to TNP-470 (5 or 20 ng/mL) and VEGF (150 ng/mL) the following day. These concentrations are based on prior experience showing that these concentrations inhibited Rho activation and migration in human microvascular endothelial cells (14). Electrical resistance was measured for 4 h. Increased permeability is indicated as a decrease in the monolayer electrical resistance.

Rac Activation. The Rac activation assay kit was purchased from Upstate Cell Signaling Solution (Lake Placid, NY) and was done according to the manufacturer's instructions. Briefly, HUVEC lysates were loaded with GTPγS (positive control) or GDP (negative control), or cells were infected with RacV12 or LacZ and then treated with VEGF (50 ng/mL) or TNP-470 (20 ng/mL). The lysates where then incubated with 10 μg Rac/cdc42 Assay Reagent (PAK-1 PBD, bound to glutathione agarose beads) per 0.5 mL of cell lysate. The proteins bound to PAK-1 PBD were separated by SDS-PAGE, transferred to nitrocellulose, and blotted with anti-Rac1 (1 μg/mL). Whole-cell lysates from the same samples were also blotted with anti-Rac to measure total Rac.

Statistical Analysis

Statistical analysis was done by using ANOVA, with significance set at $P < 0.05$.

Results

Orthotopic Model Mimics Human Anaplastic Thyroid Cancer

Following the injection of 2.5×10^5 DRO'90 cells, 90% of injected mice developed tumors that were palpable within a few days and visible by 21 days (Fig. 1B). Mice that did not develop tumors were excluded from the study. Tumors showed many histologic hallmarks of anaplastic thyroid cancer, such as extra-thyroidal extension, tracheal, and nerve invasion (Fig. 1B). In untreated mice, tumors rapidly reached sizes up to 1 g. Liver metastases observed were small and distributed through both lobes of the liver.

TNP-470 Inhibits Tumor Growth, Reduces Metastases, and Prolongs Survival in Anaplastic Thyroid Cancer

Compared with saline-treated controls, animals that received TNP-470 had significantly longer survival ($P = 0.006$; Fig. 2). Although average tumor weight at 21 days

was not significantly different between treatment groups (0.38 ± 0.08 versus 0.35 ± 0.007, respectively), gross examination of the livers revealed that TNP-470 significantly reduced visible liver metastases (16.6% versus 50%).

Tumor Proliferation and Apoptosis

To determine the effects of TNP-470 on anaplastic thyroid cancer cells, we examined tumor apoptosis by cleaved caspase-3 immunohistochemistry and cellular proliferation by staining for the nuclear Ki-67 antigen in DRO'90 tumors. DRO'90-derived tumors treated with TNP-470 showed marked increase in caspase-3 staining and decreased proliferation as measured by Ki-67 immunohistochemistry compared with tumors from untreated animals (Fig. 3A). Counterstaining with H&E and CD31 confirmed that caspase-3 and Ki-67 staining was restricted to tumor cells and not host endothelial cells. These results suggest that TNP-470 has a direct cytotoxic effect on anaplastic thyroid carcinoma cells. This is consistent with our previous data showing that TNP-470 is cytotoxic to U87 glioblastoma tumor cells at concentrations above 1 mg/mL, in contrast to its effect on endothelial cells, which occurs at much lower concentrations (14).

Tumor VEGF Levels

To determine the effect of TNP-470 on VEGF secretion, we measured VEGF levels in serum and tumor lysates. Although serum mouse VEGF levels were similar between TNP-470–treated and untreated animals (data not shown), human VEGF levels in tumor lysates were elevated in animals treated with TNP-470 (P = 0.008; Fig. 3B). This increase was not accompanied by increased microvessel density, as measured by CD31 staining (data not shown).

In vitro Experiments

To confirm the observations (increased apoptosis and reduced proliferation) in tumor sections, and to explain the lack of correlation between VEGF secretion and microvascular density, we did *in vitro* experiments to characterize the response of DRO'90 cells to TNP-470. DNA synthesis was examined using bromodeoxyuridine incorporation, whereas apoptosis was examined by ELISA for cleaved caspase-3. To confirm TNP-470–induced tumor apoptosis

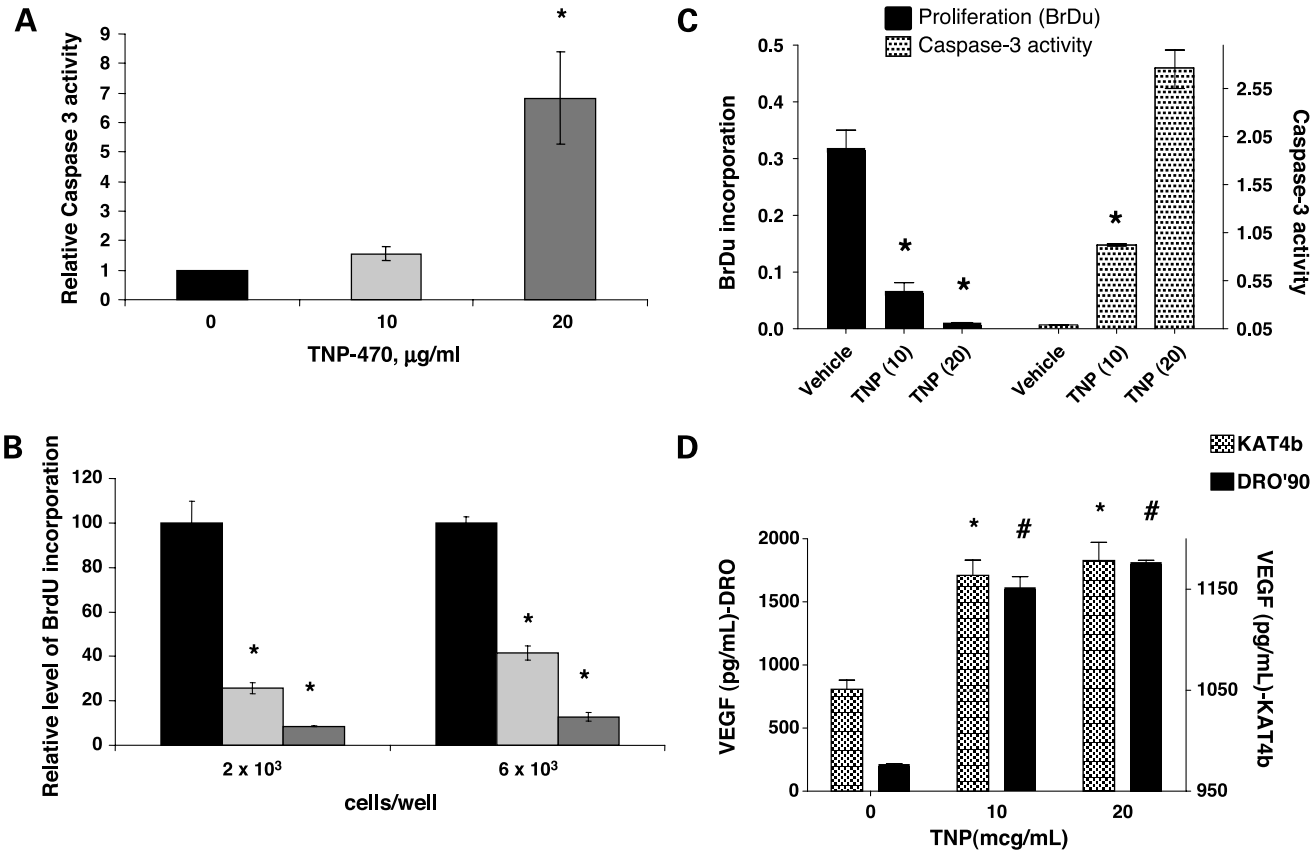

Figure 4. TNP-470 increases apoptosis, decreases proliferation, and increases secretion *in vitro*. **A,** DRO'90 cells were exposed to TNP-470 for 24 h, and apoptosis was measured by ELISA for caspase-3 activation. TNP exposure resulted in a dose-dependent increase in caspase-3 activity. **B,** cellular proliferation in DRO'90 cells was assessed by quantifying the incorporation of bromodeoxyuridine during DNA synthesis at two concentrations of cells (*black column,* vehicle controls; *light gray column,* TNP-470, 20 μg/mL; *dark gray column,* TNP-470, 40 μg/mL). TNP caused a dose-dependent decrease in DNA synthesis. *, $P < 0.05$. **C,** similar findings were observed in KAT4b cells. TNP-470 caused a similar dose-dependent increase in tumor cell apoptosis (*gray columns*) and decreased proliferation (*black columns*) in KAT4b cells *in vitro.* **D,** *in vitro* VEGF levels in supernatants from DRO'90 (*black columns*) and KAT4b (*gray columns*) cells exposed to TNP-470 (10 or 20 μg/mL). Both cell lines responded to TNP exposure by increasing VEGF secretion.

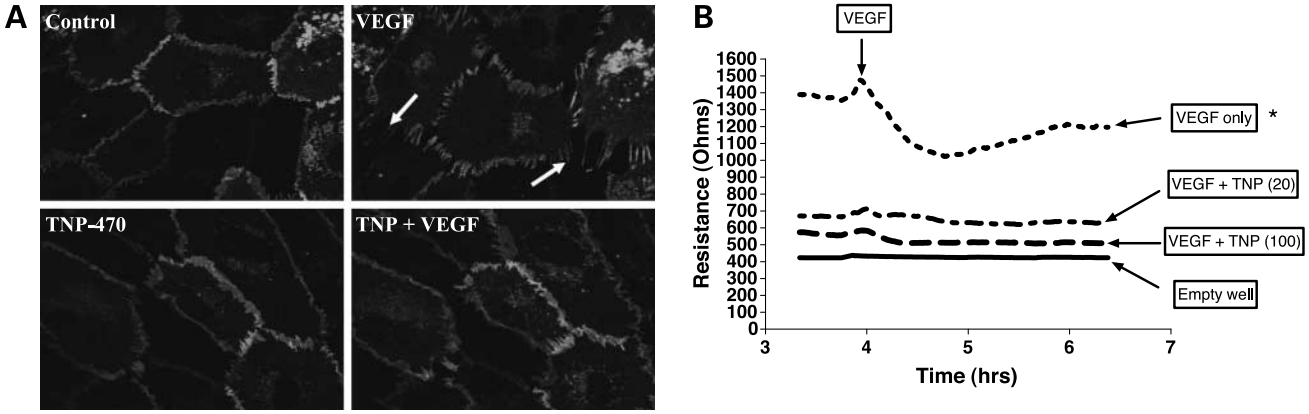

Figure 5. TNP-470 inhibits VEGF-induced intercellular gap formation and endothelial permeability. **A,** HUVEC infected with the adenoviral construct encoding full-length vascular endothelial cadherin-GFP fusion protein were exposed to TNP-470 (20 ng/mL) for 2 h followed by VEGF. Confocal microscopy images were acquired after 60 min. *Top,* intercellular gap formation after 60 min of VEGF exposure (*white arrows*). *Bottom,* absence of gap formation in monolayers exposed to both VEGF and TNP470. **B,** trans-endothelial monolayer electrical resistance was performed using the ECIS system. Confluent endothelial monolayers were exposed to TNP-470, 2 h before the addition of VEGF. VEGF (150 ng/mL) was added to all the wells except the empty control and TNP control well. The cells exposed to VEGF only showed early increase in permeability (drop in TER). TNP significantly prevented VEGF-induced endothelial permeability in a dose-dependent fashion. *, $P < 0.05$, VEGF only versus VEGF + TNP.

observed in tumor sections, we examined caspase-3 activation in DRO'90 *in vitro*. TNP-470 significantly increased apoptosis (Fig. 4A) and decreased DRO'90 proliferation *in vitro* (Fig. 4B) compared with vehicle controls ($P < 0.05$). Similar observations were present in KAT4b cells (Fig. 4C). We also exposed DRO'90 or KAT4b cells to TNP-470 or vehicle *in vitro* and measured VEGF secretion. TNP-470 markedly increased VEGF secretion by both cell types *in vitro* ($P = 0.0001$; Fig. 4D).

Endothelial Effects of TNP-470

TNP-470 Prevents VEGF-Induced Intercellular Gap Formation and Endothelial Permeability. VEGF causes endothelial proliferation, loss of homotypic adhesion, increased paracellular permeability, and endothelial migration (20, 21). Therefore, we examined the effects of TNP-470 on endothelial cell-cell adhesion and permeability. Vascular endothelial cadherin is the main component of endothelial adherens junctions, which regulate endothelial homotypic adhesion and barrier function (22). We overexpressed vascular endothelial cadherin by infecting HUVEC with an adenoviral vector coding for a vascular endothelial cadherin-GFP fusion protein, which enables live-cell imaging by confocal microscopy. The cells were then exposed to VEGF (50 ng/mL) in the presence or absence of TNP-470. TNP-470 prevented VEGF-induced intercellular gap formation (Fig. 5A) and increased EC permeability in a dose-dependent manner (Fig. 5B).

TNP-470 Prevents VEGF-Induced Endothelial Cytoskeletal Changes and Ruffles. VEGF-induced endothelial migration is associated with morphologic changes in the actin cytoskeleton and ruffle formation (20, 21). Therefore, we examined the effect of TNP-470 on VEGF-induced stress fiber and ruffle formation. HUVEC infected with adenoviral actin-GFP were exposed to VEGF (50 ng/mL) in the presence or absence of TNP-470 (20 ng/mL). Using confocal microscopy, we observed marked increase in endothelial stress fibers 30 min after VEGF exposure (Fig. 6A, *top right*). This was associated with formation of actin-rich ruffles at the leading edge of migrating cells. TNP-470 prevented both VEGF-induced ruffle formation and the changes in the endothelial cytoskeleton and cell morphology (Fig. 6A, *bottom right*).

Rac Activation

Rac activation is associated with ruffle formation and endothelial migration (15, 23). Therefore, we examined the effects of TNP-470 on endothelial Rac activation. HUVEC were infected with adenoviral actin-GFP in combination with adenoviral constructs coding for the dominant-negative RacN17 or constitutively active RacV12. Cells were then exposed to VEGF in the presence or absence of TNP-470. Dominant-negative RacN17 prevented VEGF-induced ruffle formation (Fig. 6B, *top right*), whereas treatment with TNP-470 blocks ruffle formation induced by the constitutively active RacV12 (Fig. 6B, *bottom right*). In addition, we show that TNP-470 inhibits Rac activation induced by RacV12 (Fig. 6C).

Discussion

In this study, we show that TNP-470 inhibits proliferation of anaplastic thyroid carcinoma cells and prolongs survival in an orthotopic mouse model. Furthermore, TNP-470 increased tumor cell apoptosis, decreased proliferation in two different human anaplastic thyroid cancer cell lines, and prevented VEGF-induced endothelial cell-cell adhesion, ruffle formation, and cytoskeletal changes. The latter effects seem to be Rac dependent. Anaplastic thyroid cancer accounts for approximately one quarter of the deaths from thyroid cancer. At the time of presentation, more than three quarters of patients have lymph node

metastases, and 50% have distant metastases (24). Most patients present with large tumors, and the average survival is less than 1 year, making this the most aggressive subtype of thyroid cancer. A major challenge in developing effective therapy is the relative lack of clinically relevant animal models in anaplastic thyroid cancer. S.c. xenograft models are a popular method used to study human cancers; however, there is evidence that orthotopic models more closely mimic the tumor microenvironment (and is more clinically relevant) in human cancer (8, 9). Kim et al. previously showed the feasibility of an orthotopic thyroid cancer model (18). Similarly, our model shows a high tumor take (90%) in a short period. These tumors have similar characteristics to human anaplastic thyroid cancer, including local invasion, metastases, and high mortality. These characteristics are important if we are to develop effective therapy in animal models.

Tumor angiogenesis is an important process that facilitates the growth and metastases of tumors, including thyroid cancer (1, 24) Anaplastic thyroid cancer cells produce endothelial growth factors, and antiangiogenic strategies reduce thyroid cancer growth *in vitro* and *in vivo*

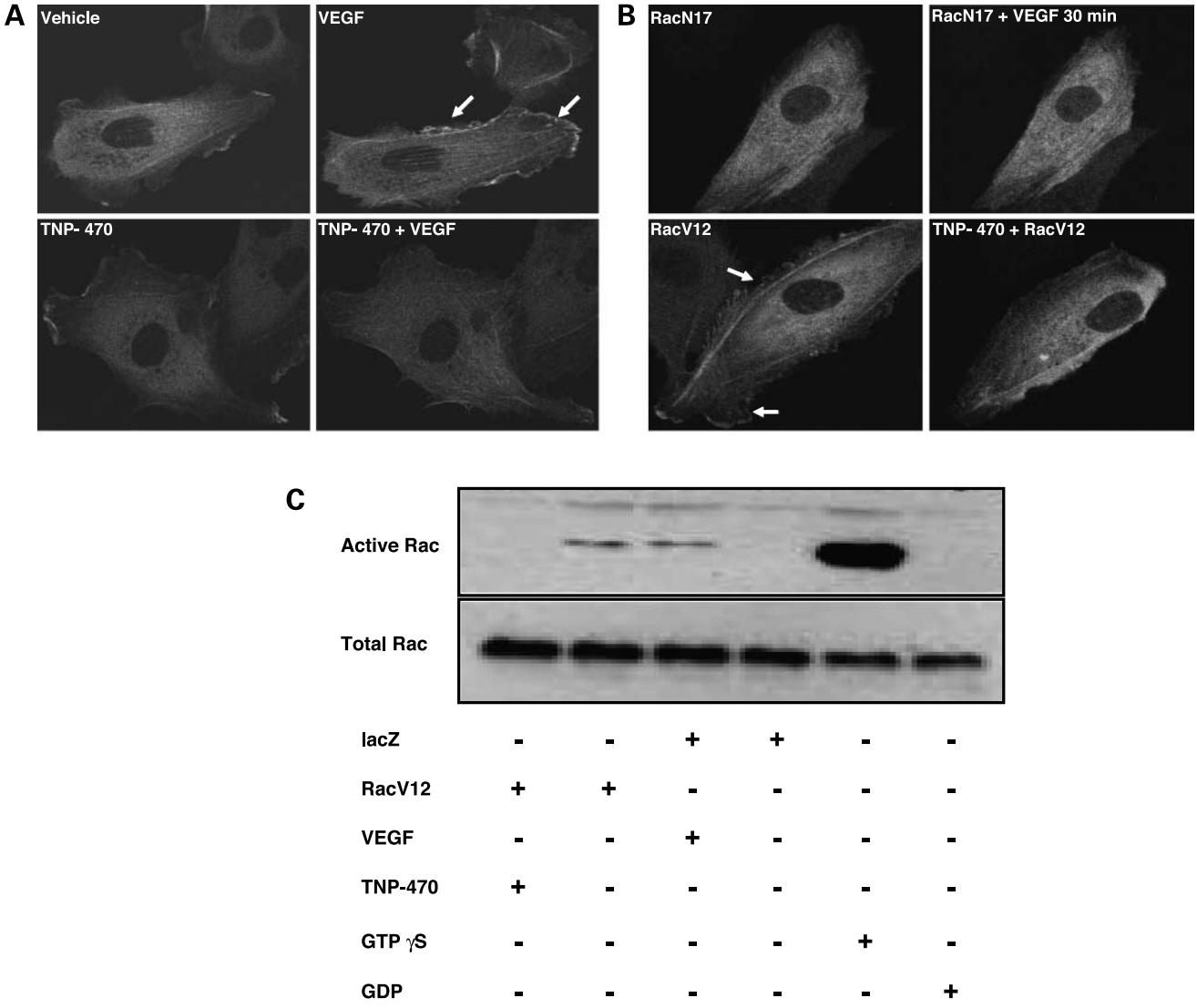

Figure 6. TNP-470 prevents Rac-dependent ruffle formation. **A,** HUVEC were infected with an adenovirus construct encoding actin-GFP fusion protein. Endothelial cells were then exposed to TNP-470 (20 ng/mL) for 2 h followed by VEGF exposure (50 ng/mL). Confocal microscopy images were acquired after 30 min. VEGF exposure caused ruffle formation and prominent actin stress fibers (*top right*). In contrast, TNP-470 prevented VEGF-induced ruffle formation (*bottom right*). **B,** HUVEC were coinfected with an adenovirus construct encoding actin-GFP fusion protein and either the dominant-negative RacN17 mutation or the constitutively active RacV12 mutation. RacN17 prevented VEGF-induced ruffle formation (*top right*), whereas TNP470 prevented RacV12-induced ruffle formation (*bottom right*). **C,** HUVEC were infected with RacV12 (*lanes 1* and *2*) or Lac Z (*lanes 3* and *4*). After 24 h, cells were exposed to TNP-470 (20 ng/mL; *lane 1*) or VEGF (50 ng/mL; *lane 3*) then lysed, and Rac activation was determined. RacV12- and VEGF-activated Rac (*lanes 2* and *3*, respectively). TNP-470 prevented RacV12-induced Rac activation. *Lane 5,* positive control; *lane 6,* negative control.

(2, 3, 7, 25). In fact, serum levels of proangiogenesis factors such as VEGF are elevated in patients with thyroid cancer and decrease after surgical resection (6). Others have also suggested that angiogenesis inhibition may the mechanism of action of some modestly effective chemotherapeutic agents for thyroid cancer (26, 27). These observations suggest that the use of angiogenesis inhibitors may be a viable therapeutic strategy for patients with anaplastic thyroid cancer. TNP-470 [*O*-(chloroacetyl-carbamoyl) fumagillol, AGM-1470] was initially derived from fumagillin and has potent antiangiogenic effects in many tumors (10, 11, 28–31). TNP-470 reduces tumor size in pancreatic (29, 32), bladder (33), and cervical and prostate cancer (34). However, few studies have examined the intracellular pathways that mediate the endothelial effects of TNP- 470. Even fewer studies report on non-endothelial mechanisms of TNP-470–induced reduction in tumor growth. One generally accepted hypothesis is that growth-inhibiting effects of TNP-470 are due to a reduction in endothelial proliferation and angiogenesis. We previously showed that TNP-470 inhibits vascular hyperpermeability of tumor blood vessels and VEGF-induced migration of endothelial cells, both important steps in tumor angiogenesis (14). In this study, we extend those findings by examination of the mechanisms of TNP-470 effects on cytoskeletal pathways in endothelial cells. The RhoA family of small GTPases, including rho, rac, and cdc42, has been shown to regulate changes in cell morphology, adhesion, motility, and mitogen-activated protein kinase activation. Rho proteins also regulate cytoskeletal reorganization and the integrity of intercellular junctions (15, 23). We previously reported that TNP-470 inhibits RhoA activation (14). Because both RhoA and Rac1 are required for VEGF receptor-2–mediated endothelial migration (35), and because Rac is known to cause cytoskeletal changes (16), we hypothesized that TNP-470 impairs endothelial migration by a Rac-dependent mechanism.

In the current study, we implicate Rac as a mediator of VEGF-induced endothelial stress fibers and ruffle formation, and implicate Rac inhibition as a mechanism for antiangiogenic effects of TNP-470. TNP-470 also prevented VEGF-induced loss of endothelial cell homotypic adhesion, a process that is necessary for endothelial migration and angiogenesis (36). It is unclear from our studies whether the loss of homotypic adhesion is the consequence of cytoskeletal changes, or if it occurs independently of the cytoskeleton. The observed intercellular gap formation associated with endothelial cell-cell adhesion may have consequences for increased tumor interstitial pressure and bioavailability of chemotherapeutic agents given during combination therapy.

Although much is known about the effects of TNP-470 on endothelium, there are few reports on direct tumor cell effects of TNP-470. Huang et al. showed that TNP-470 was directly cytotoxic to Wilm's tumor cells (37). We found increased apoptosis and decreased tumor cell proliferation after TNP-470 exposure. However, the concentrations of TNP-470 that caused tumor cell apoptosis in this study were higher that those reported to cause endothelial apoptosis (13). Therefore, the observed tumor cell toxicity *in vivo* could be secondary to *in vivo* endothelial toxicity. However, others have suggested that the chemotherapeutic agents manumycin and paclitaxel may inhibit anaplastic thyroid tumor growth by enhancing tumor apoptosis, regardless of the observed endothelial effects (26, 27, 38). We also observed that tumor VEGF levels were higher in animals that received TNP-470 compared with the control group. This was confirmed by *in vitro* experiments in both DRO'90 and KAT4b cells. Although this seems counterintuitive, increased VEGF levels following TNP-470 exposure have been reported in prostate cancer (28) and in SSC leg bearing mice (39). We speculate that the increased VEGF expression is a result of TNP-470–induced stress on the tumor cells. The mechanisms of such stress remain to be determined. We observed overlap between the concentrations of TNP-470, which caused apoptosis, and those that increased VEGF secretion from tumor cells *in vitro*. This may be partially explained by the possibility that the range of concentrations of TNP-470 used may not result in uniform cell death in our cell cultures; therefore, the surviving anaplastic thyroid carcinoma cells may respond to the TNP-induced stress by increasing VEGF secretion. However, the implication is that TNP-470 may be best administered as part of combination therapy. Specifically TNP-470 may act synergistically with other agents that prevent VEGF production by tumor cells or sequester secreted VEGF, such as Avastin, a monoclonal antibody to VEGF (40).

The concentrations of TNP-470 used for our *in vitro* studies (5–20 ng/mL) are similar to those achieved in clinical trials (41, 42), which show that serum TNP levels > 477 ng/mL are not toxic. The concentration used for *in vivo* studies have also been used in prior experiments with no toxicity in mice (13, 14). In clinical trials, TNP toxicity is predominantly neurologic and has been attributed to accumulation of TNP-470 in brain tissue. Many of the observed toxic effects of TNP-470 have been prevented by the newer polymer conjugate caplostatin, which is unable to cross the blood-brain barrier (13, 14).

We did not seek to determine the specific molecules that mediate TNP effects on endothelium (Rac pathway) or tumors (apoptosis). There are no confirmed molecular targets of TNP-470; therefore, the identification of molecular targets of antiangiogenic agents such as TNP-470 represents an important question that will form the basis of future experiments. Identifying such targets will greatly facilitate the development of improved antiangiogenic agents and determining the causes of ''resistance'' to antiangiogenic agents.

We have shown that TNP-470 inhibits tumor growth and metastases and prolongs survival in orthotopic mouse model of anaplastic thyroid cancer. These findings argue for the use of TNP-470 in combination with other agents that prevent VEGF production by tumor cells. We predict that such approaches will improve the therapeutic effects of antiangiogenic agents such as TNP-470.

Acknowledgments

We thank Jeffery M. Stark and Christa L. Hladik for valuable technical assistance.

References

1. Pasieka JL. Anaplastic thyroid cancer. Curr Opin Oncol 2003;15:78–83.

2. Poulaki V, Mitsiades CS, McMullan C, et al. Regulation of vascular endothelial growth factor expression by insulin-like growth factor I in thyroid carcinomas. J Clin Endocrinol Metab 2003;88:5392–8.

3. Schoenberger J, Grimm D, Kossmehl P, Infanger M, Kurth E, Eilles C. Effects of PTK787/ZK222584, a tyrosine kinase inhibitor, on the growth of a poorly differentiated thyroid carcinoma: an animal study. Endocrinology 2004;145:1031–8.

4. Katoh R, Miyagi E, Kawaoi A, et al. Expression of vascular endothelial growth factor (VEGF) in human thyroid neoplasms. Hum Pathol 1999;30:891–7.

5. Bunone G, Vigneri P, Mariani L, et al. Expression of angiogenesis stimulators and inhibitors in human thyroid tumors and correlation with clinical pathological features. Am J Pathol 1999;155:1967–76.

6. Tuttle RM, Fleisher M, Francis GL, Robbins RJ. Serum vascular endothelial growth factor levels are elevated in metastatic differentiated thyroid cancer but not increased by short-term TSH stimulation. J Clin Endocrinol Metab 2002;87:1737–42.

7. Bauer AJ, Terrell R, Doniparthi NK, et al. Vascular endothelial growth factor monoclonal antibody inhibits growth of anaplastic thyroid cancer xenografts in nude mice. Thyroid 2002;12:953–61.

8. Killion JJ, Radinsky R, Fidler IJ. Orthotopic models are necessary to predict therapy of transplantable tumors in mice. Cancer Metastasis Rev 1998;17:279–84.

9. Bibby MC. Orthotopic models of cancer for preclinical drug evaluation: advantages and disadvantages. Eur J Cancer 2004;40:852–7.

10. Kusaka M, Sudo K, Matsutani E, et al. Cytostatic inhibition of endothelial cell growth by the angiogenesis inhibitor TNP-470 (AGM-1470). Br J Cancer 1994;69:212–6.

11. Ingber D, Fujita T, Kishimoto S, et al. Synthetic analogues of fumagillin that inhibit angiogenesis and suppress tumour growth. Nature 1990;348:555–7.

12. Kudelka AP, Verschraegen CF, Loyer E. Complete remission of metastatic cervical cancer with the angiogenesis inhibitor TNP-470. N Engl J Med 1998;338:991–2.

13. Satchi-Fainaro R, Puder M, Davies JW, et al. Targeting angiogenesis with a conjugate of HPMA copolymer and TNP-470. Nat Med 2004;10:255–61.

14. Satchi-Fainaro R, Mamluk R, Wang L, et al. Inhibition of vessel permeability by TNP470 and its polymer conjugate, caplostatin. Cancer Cell 2005;7:251–61.

15. Van Hennik PB, Hordijk PL. Rho GTPases in hematopoietic cells. Antioxid Redox Signal 2005;7:1440–55.

16. van Wetering S, van Buul JD, Quik S, et al. Reactive oxygen species mediate Rac induced loss of cell-cell adhesion in primary human endothelial cells. J Cell Sci 2002;115:1837–46.

17. Foukakis T, Thoppe SR, Lagercrantz S, et al. Molecular cytogenetic characterization of primary cultures and established cell lines from non-medullary thyroid tumors. Int J Oncol 2005;26:141–9.

18. Kim S, Park YW, Schiff BA, et al. An orthotopic model of anaplastic thyroid carcinoma in athymic nude mice. Clin Cancer Res 2005;11:1713–21.

19. Nwariaku FE, Liu Z, Zhu X, et al. The NADPH oxidase mediates vascular endothelial cadherin phosphorylation and endothelial dysfunction. Blood 2004;104:3214–20.

20. Dye J, Lawrence L, Linge C, Leach L, Firth J, Clark P. Distinct patterns of microvascular endothelial cell morphology are determined by extracellular matrix composition. Endothelium 2004;11:151–67.

21. Gerhardt H, Golding M, Fruttiger M, et al. VEGF guides angiogenic sprouting utilizing endothelial tip cell filopodia. J Cell Biol 2003;161:1163–77.

22. Carmeliet P, Collen D. Molecular basis of angiogenesis. Role of VEGF and VEcadherin. Ann N Y Acad Sci 2000;902:249–62.

23. Hordijk P. Endothelial signaling in leukocyte transmigration. Cell Biochem Biophys 2003;38:305–22.

24. Are C, Shaha AR. Anaplastic thyroid carcinoma: biology, pathogenesis, prognostic factors, and treatment approaches. Ann Surg Oncol 2006;13:453–64.

25. Bauer AJ, Patel A, Terrell R, et al. Systemic administration of vascular endothelial growth factor monoclonal antibody reduces the growth of papillary thyroid carcinoma in a nude mouse model. Ann Clin Lab Sci 2003;33:192–9.

26. Yeung SC, Xu G, Pan J, Christgen M, Bamiagis A. Manumycin enhances the cytotoxic effect of paclitaxel on anaplastic thyroid carcinoma cells. Cancer Res 2000;60:650–6.

27. Xu G, Pan J, Martin C, Yeung SC. Angiogenesis inhibition in the *in vivo* antineoplastic effect of manumycin and paclitaxel against anaplastic thyroid carcinoma. J Clin Endocrinol Metab 2001;86:1769–77.

28. Bhujwalla ZM, Artemov D, Natarajan K, Solaiyappan M, Kollars P, Kristjansen PEG. Reduction of vascular and permeable regions in solid tumors detected by macromolecular contrast magnetic resonance imaging after treatment with antiangiogenic agent TNP-470. Clin Cancer Res 2003;9:355–62.

29. Hotz HG, Reber HA, Hotz B, et al. Angiogenesis inhibitor TNP-470 reduces human pancreatic cancer growth. J Gastrointest Surg 2001;5:131–8.

30. Mysliwski A, Koszalka P, Bigda J, Szmit E. Complete remission of Bomirski Ab amelanotic melanoma in hamsters treated with the angiogenesis inhibitor TNP-470. Neoplasma 2002;49:319–22.

31. Mysliwski A, Kubasik-Juraniec J, Koszalka P, Szmit E. The effect of angiogenesis inhibitor TNP-470 on the blood vessels of the lungs, kidneys and livers of treated hamsters. Folia Morphol (Warsz) 2004;63:5–9.

32. Junichi Miyazaki YT, Matsuzaki K, Hokari R, et al. Combination therapy with tumor-lysate pulsed dendritic cells and antiangiogenic drug TNP-470 for mouse pancreatic cancer. Int J Cancer 2005;117:499–505.

33. Muramaki M, Miyake H, Hara I, Kawabata G, Kamidono S. Synergistic inhibition of tumor growth and metastasis by combined treatment with TNP-470 and gemcitabine in a human bladder cancer KoTCC-1 model. J Urol 2004;172:1485–9.

34. Muramaki M, Miyake H, Hara I, Kamidono S. Synergistic inhibition of tumor growth and metastasis by combined treatment with TNP-470 and docetaxel in a human prostate cancer PC-3 model. Int J Oncol 2005;26:623–8.

35. Zeng H, Zhao D, Mukhopadhyay D. KDR stimulates endothelial cell migration through heterotrimeric G protein Gq/11-mediated activation of a small GTPase RhoA. J Biol Chem 2002;277:46791–8.

36. Dejana E, Lampugnani MG, Martinez-Estrada O, Bazzoni G. The molecular organization of endothelial junctions and their functional role in vascular morphogenesis and permeability. Int J Dev Biol 2000;44:743–8.

37. Huang J, Frischer JS, New T, et al. TNP-470 promotes initial vascular sprouting in xenograft tumors. Mol Cancer Ther 2004;3:335–43.

38. Pan J, Huang H, Sun L, Fang B, Yeung SC. Bcl-2-associated X protein is the main mediator of manumycin a-induced apoptosis in anaplastic thyroid cancer cells. J Clin Endocrinol Metab 2005;90:3583–91.

39. Kanamori S, Nishimura Y, Okuno Y, Horii N, Saga T, Hiraoka M. Induction of vascular endothelial growth factor (VEGF) by hyperthermia and/or an angiogenesis inhibitor. Int J Hyperthermia 1999;15:267–78.

40. Satchi-Fainaro R, Butterfield C, Akslen L, Short S, Folkman J. HPMA copolymer-TNP-470 (caplostatin) and Avastin show synergistic inhibition of human tumor growth in mice. Eur J Cancer Suppl 2005;3:15.

41. Bhargava P, Marshall JL, Rizvi N, et al. A phase I and pharmacokinetic study of TNP-470 administered weekly to patients with advanced cancer. Clin Cancer Res 1999;5:1989–95.

42. Tran HT, Blumenschein GR, Jr., Lu C, et al. Clinical and pharmacokinetic study of TNP-470, an angiogenesis inhibitor, in combination with paclitaxel and carboplatin in patients with solid tumors. Cancer Chemother Pharmacol 2004;54:308–14.